SIMULATION OF THE OPERATION OF THE CAR RADIATOR WITH A LAMINAR, TRANSITIONAL, AND TURBULENT REGIME OF LIQUID FLOW IN THE TUBES

by

Dawid TALER*

Department of Thermal Processes, Air Protection and Waste Utilization,
Faculty of Environmental Engineering, The Cracow University of Technology,
Cracow, Poland

Original scientific paper
https://doi.org/10.2298/TSCI19S4311T

The results of the simulation of car radiator operation with a large range of changes in the volume flow rate of liquid inside the tubes were presented. The change of the flow regime from laminar through transitional to turbulent flow was taken into account. Semi-empirical and empirical relationships for the Nusselt number on the liquid-side in the laminar, transitional, and turbulent range were used. The Nusselt number on the air side was determined using empirical power-type correlation. The friction factor in the transition flow range was calculated by linear interpolation between the values of the friction factor for the Reynolds number equal to 2100 and 3000. The water and air temperature at the outlet of the heat exchanger were calculated using effectiveness-number of transfer units method. The heat-flow rate from water to air was calculated as a function of the water-flow rate to compare it with the experimental results. The calculation results agreed very well with the results of the measurements.

Keywords: *plate fin-and-tube heat exchanger, friction factor, heat-flow rate, laminar, transition, and turbulent flow in tubes, experimental test air- and water-side heat transfer correlation*

Introduction

Finned heat exchangers are used when one fluid is a gas and the liquid flows inside the tubes. The fins are attached to the tubes. Water heaters, evaporators, and superheaters in heat recovery steam generators are usually made of finned tubes. Heat exchangers with tubes finned by individual or continuous fins are the essential equipment in dry cooling systems used to cool water in power stations [1-3]. Plate-fin and tube heat exchangers (PFTHE) are widely used as car radiators and car air heaters. Also, PFTHE are very widespread in ventilation, and air-conditioning systems. The intensive development of RES favors the development of PFTHE. The exchangers in such installations are characterized by low load operation when velocities of the air-flowing perpendicular to the tube axis and liquid flowing inside the tube are low. Thermohydraulic fundamentals, design, and fabrication of heat exchangers, including PFTHE, are described in the book of Kuppan [2]. Many enhanced air-side surfaces such as

* Author's e-mail: dtaler@pk.edu.pl

various wavy plate fins and louvered fins are discussed. Also, different techniques for intensifying the heat transfer inside the tubes are presented.

In the design calculations of heat exchangers, the logarithmic mean temperature difference (LMTD) method is most commonly used [1-3]. In the performance calculations of PFTHE, the ε-NTU or P-NTU methods are widely used for non-iterative calculations of the temperature of both fluids at the outlet of the PFTHE. The symbols ε and P denote the effectiveness of the heat exchanger, and the NTU denotes the number of transfer units. Formulas and diagrams for ε(NTU) and P(NTU) for PFTHE with various flow arrangements with a different number of passes are presented by Kuppan [2]. The outlet temperatures of both fluids can easily be calculated using the formulas for calculating ε or P for a given NTU value. If the exchanger arrangement is complicated and there are no formulas for calculating the effectiveness ε or P, then the numerical model of the PFTHE exchanger can be constructed using the method developed by Taler [3, 4]. Heat transfer correlations for calculating heat transfer coefficients on both air and water side are needed in the thermal calculations of heat exchangers using engineering methods such as LMTD, ε-NTU, and P-NTU. These correlations are also required in the finite difference model developed in [3, 4].

The most frequently used relationships for calculating the liquid-side heat transfer coefficient for turbulent flow are the Dittus-Boelter, see [5], or Gnielinski [6] correlations suitable only for high Reynolds numbers when the Re_w is larger than 4000. Using the Dittus-Boelter relationship for smaller values of Reynolds numbers for flow in tubes leads to too high heat transfer coefficients and in consequence to excessive heat-flow rates transferred in PFTHE from hot water to air.

The transitional flow regime in long tubes with a smooth inner surface was extensively investigated by Ghajar and Tam [7] and by Everts and Meyer [8]. The pressure drops and heat transfer measurements in the transition region for a circular tube with three different inlet configurations: squared-edged, re-entrant, and bell-mouth were determined by Ghajar and Tam.

Recently, Taler [9] proposed a new correlation to calculate the Nusselt number for the transitional and turbulent fluid-flow inside the tubes at a given tube surface temperature or constant heat flux.

The heat transfer coefficient on the air side is usually determined using empirical power correlations. Recently, air-side heat transfer correlations in PFTHE were also determined by CFD simulation. Due to the low computing power of modern computers, flow and heat transfer were only modeled on the air side. The temperature of the outer or inner surface of the tubes and even of the whole fins was assumed to be uniform. The flow of air was modeled as laminar or turbulent using different turbulence models. A brief review of articles on determining the correlations for calculating the Nusselt number on the air side was presented by Taler [10].

A mathematical model of the heat exchanger

Performance calculations of the investigated PFTHE, *i. e.*, determining the temperature of the water and air at the outlets of the investigated heat exchanger were conducted using the P-NTU method.

Thermohydraulic tests of air-cooled plate fin-and-tube heat exchanger were carried out in a laminar, transition and turbulent flow regime of water in the tubes. The tested PFTHE was a car radiator for a spark engine with a displacement volume of 1600 [cm^3] [11]. Two-pass car radiator has two rows of round tubes. There are twenty tubes in the first pass, ten in

each row, *i. e.* $n_u = 10$. The number of tubes in the second pass is smaller and is eighteen, nine in each row, *i. e.* $n_l = 9$.The tube arrangement is in-line. Water-flows in parallel through the first and second row of tubes in both first and second pass. Between the first and second pass, there is a chamber in which water from the first and second row of tubes is mixed and then flows into the second pass. The flow arrangement of an automobile radiator is shown in fig. 1.

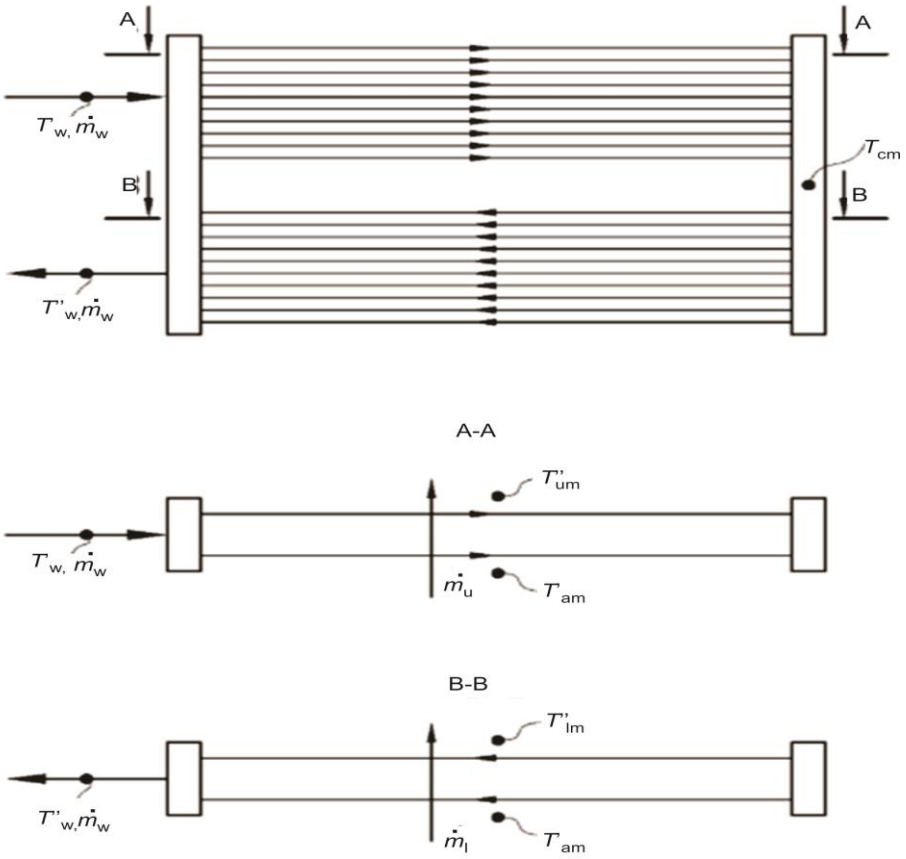

Figure 1. Flow arrangement of the two-row, two-pass car radiator with front and top view

The internal diameter of the tube with the wall thickness $\delta_t = 0.5$ mm is $d_{in} = 6.2$ mm. The transverse pitch of the tube arrangement is equal to $p_1 = 18.5$ mm, and the longitudinal pitch is $p_2 = 12$ mm. The plate fins with a thickness of 0.08 mm are set on tubes with the pitch of 1.5 mm. Dimensions of the heat exchanger are as follows: length $L_{ch} = 520$ mm, height $H_{ch} = 359$ mm, and thickness $W_{ch} = 2p_2 = 24$ mm. The mean water, T_{cm}, and air temperature, T'''_{um}, after the first pass and after the second pass T''_w and T'''_{lm}, fig. 1, were calculated using the *P*-NTU method. Formulas for calculating the water-side effectiveness, P_w, and air-side effectiveness, P_a, were derived based on the mathematical model of the heat exchanger developed by Taler [12]. The numbers of heat transfer units for water NTU_w and air NTU_a are defined in relation to one tube located in the first (upper) or second (lower) pass. The numbers of transfer units are:

First (upper) pass

$$N_{\mathrm{a,u}} = \frac{U_{o,\mathrm{u}}\, A_o}{\dot{m}_{\mathrm{a,t}}\, \overline{c}_{p,\mathrm{a}}}, \quad N_{\mathrm{w,u}} = \frac{U_{o,\mathrm{u}}\, A_o}{\dot{m}^{u}_{\mathrm{w,t}}\, \overline{c}_{p,\mathrm{w}}} \tag{1}$$

Second (lower) pass

$$N_{\mathrm{a,l}} = \frac{U_{o,\mathrm{l}}\, A_o}{\dot{m}_{a,\mathrm{t}}\, \overline{c}_{p,\mathrm{a}}}, \quad N_{\mathrm{w,l}} = \frac{U_{o,\mathrm{l}}\, A_o}{\dot{m}^{l}_{w,\mathrm{t}}\, \overline{c}_{p,\mathrm{w}}} \tag{2}$$

The mass-flow rate $\dot{m}_{a,\mathrm{t}} = w_0\, p_2\, L_{\mathrm{ch}}\, \rho_{\mathrm{a}}\big|_{T'_{\mathrm{am}}}$ in eqs. (1) and (2) denotes the air mass-flow rate per one pitch p_2 (through the cross-section $p_2 L_{\mathrm{ch}}$). Similarly, the water mass-flow rates $\dot{m}^{u}_{\mathrm{w,t}}$ and $\dot{m}^{l}_{\mathrm{w,t}}$ per one tube are $\dot{m}^{u}_{\mathrm{w,t}} = \dot{m}_{\mathrm{w}} / (2n_u)$ and $\dot{m}^{l}_{\mathrm{w,t}} = \dot{m}_{\mathrm{w}} / (2n_l)$, respectively.

The air and water side effectiveness of the first pass is defined by:

$$P_{\mathrm{a,u}} = \frac{T'''_{\mathrm{um}} - T'_{\mathrm{am}}}{T'_{\mathrm{w}} - T'_{\mathrm{am}}}, \quad P_{\mathrm{w,u}} = \frac{T_{\mathrm{cm}} - T'}{T'_{\mathrm{w}} - T'_{\mathrm{am}}} \tag{3}$$

The following formulas were obtained using the mathematical model of the exchanger presented in the paper [12]:

$$P_{\mathrm{a,u}} = \left(1 - \mathrm{e}^{-N_{a,u}}\right)^2 \left(\frac{1 - \mathrm{e}^{-B_u}}{B_u} - \mathrm{e}^{-B_u}\right) + \left(1 - \mathrm{e}^{-2N_{a,u}}\right) \frac{1 - \mathrm{e}^{-B_u}}{B_u} \tag{4}$$

$$P_{\mathrm{w,u}} = 1 - \mathrm{e}^{-B_u} - \frac{N_{\mathrm{w,u}}}{2N_{\mathrm{a,u}}} \left(1 - \mathrm{e}^{-N_{a,u}}\right)^2 \mathrm{e}^{-B_u} \tag{5}$$

where the symbol B_u denotes:

$$B_u = \frac{N_{\mathrm{w,u}}}{N_{\mathrm{a,u}}} \left(1 - \mathrm{e}^{-N_{a,u}}\right) \tag{6}$$

The water temperature, T_{cm}, at the outlet from the first pass as well as the average air temperature T'''_{um} after the first pass can be determined using only the eq. (3) for water-side effectiveness $P_{\mathrm{w,u}}$. The temperature, T_{cm}, can be obtained from the definition (3):

$$T_{cm} = T'_{\mathrm{w}} - P_{\mathrm{w,u}} \left(T'_{\mathrm{w}} - T'_{am}\right) \tag{7}$$

where $P_{\mathrm{w,u}}$ is calculated using the relationship (5).

Solving the heat balance equation for the upper pass gives the air temperature T'''_{um}:

$$T'''_{um} = T'_{am} + \dot{m}_w\, \overline{c}_w \frac{T'_w - T_{cm}}{\dot{m}_u\, \overline{c}_{p,\mathrm{a}}} \tag{8}$$

The air mass-flow rate $\dot{m}_u$ through the upper heat exchanger pass is:

$$\dot{m}_u = \frac{\dot{m}_a\, n_u}{n_u + n_l} \tag{9}$$

With the known temperature T_{cm}, the liquid temperature T''_w at the heat exchanger outlet and the air mean temperature T'''_{lm} behind the second pass can be determined similarly. The air-side and water side-effectiveness of the second pass is defined:

$$P_{\mathrm{a,l}} = \frac{T'''_{lm} - T'_{am}}{T_{cm} - T'_{am}}, \quad P_{\mathrm{w,l}} = \frac{T_{cm} - T''}{T_{cm} - T'_{am}} \tag{10}$$

The relationships for $P_{\mathrm{a,l}}$ and $P_{\mathrm{w,l}}$ are:

$$P_{\mathrm{a,l}} = \left(1-\mathrm{e}^{-N_{a,l}}\right)^2 \left(\frac{1-\mathrm{e}^{-B_l}}{B_l} - \mathrm{e}^{-B_l}\right) + \left(1-\mathrm{e}^{-2N_{a,l}}\right)\frac{1-\mathrm{e}^{-B_l}}{B_l} \tag{11}$$

$$P_{\mathrm{w,l}} = 1-\mathrm{e}^{-B_l} - \frac{N_{\mathrm{w,l}}}{2N_{\mathrm{a,l}}}\left(1-\mathrm{e}^{-N_{\mathrm{a,l}}}\right)^2 \mathrm{e}^{-B_l} \tag{12}$$

where the symbol B_l denotes:

$$B_l = \frac{N_{\mathrm{w,l}}}{N_{\mathrm{a,l}}}\left(1-\mathrm{e}^{-N_{\mathrm{a,l}}}\right) \tag{13}$$

The water temperature T_w'' at the outlet from the second pass and the average air temperature T_{lm}''' after the second pass can be determined using the relationships for the water-side effectiveness $P_{\mathrm{w,l}}$ and air-side effectiveness $P_{\mathrm{a,l}}$. The water temperature T_w'' at the outlet from the second pass is:

$$T_w'' = T_{cm} - P_{\mathrm{w,l}}\left(T_{cm} - T_{am}'\right) \tag{14}$$

where $P_{\mathrm{w,l}}$ is given by eq. (12).

Solving the heat balance equation for the second pass gives the mean air temperature T_{lm}''' after the second pass:

$$T_{lm}''' = T_{am}' + \dot{m}_w \bar{c}_w \frac{T_{cm} - T_w^{"}}{\dot{m}_l \bar{c}_{p,a}} \tag{15}$$

The air mass-flow rate $\dot{m}_l$ through the lower (second) heat exchanger pass is:

$$\dot{m}_l = \frac{\dot{m}_a n_l}{n_u + n_l} \tag{16}$$

The mean temperature of the air T_{am}'' after the heat exchanger is calculated from the formula:

$$T_{am}'' = \frac{n_u T_{um}'''}{n_u + n_l} + \frac{n_l T_{lm}'''}{n_u + n_l} \tag{17}$$

If the temperature of the water T_w'' at the exit from the heat exchanger is known, then the temperature of the air after the heat exchanger T_{am}'' can also be determined from the heat balance equation for the exchanger, fig. 1:

$$T_{am}'' = T_{am}' + \dot{m}_w \bar{c}_w \frac{T_w' - T_w''}{\dot{m}_a \bar{c}_{p,a}} \tag{18}$$

The presented procedure for calculating the water and air outlet temperature based on the *P*-NTU method can also be applied to other types of heat exchangers with different flow systems. Many relationships for calculating the effectiveness, *P*, as a function of the NTU can be found in the books on the heat exchangers [1-3]. Overall heat transfer coefficients $h_{o,\mathrm{l}}$ and $h_{o,\mathrm{u}}$ referred to the outer surface area of the bare tube for the lower and upper pass are given by:

$$\frac{1}{U_{o,\mathrm{l}}} = \frac{1}{h_{\mathrm{w,l}}}\frac{r_o}{r_{\mathrm{in}}} + \frac{r_o}{k_{\mathrm{t}}}\ln\left(\frac{r_o}{r_{\mathrm{in}}}\right) + \frac{1}{h_o}, \quad \frac{1}{U_{o,\mathrm{u}}} = \frac{1}{h_{\mathrm{w,u}}}\frac{r_o}{r_{\mathrm{in}}} + \frac{r_o}{k_{\mathrm{t}}}\ln\left(\frac{r_o}{r_{\mathrm{in}}}\right) + \frac{1}{h_o} \tag{19}$$

The effective heat transfer coefficient h_o taking into account the presence of fins, based on the surface area of the bare tube was determined using the following relationship:

$$h_o = \left(\frac{A_{bf}}{A_o} + \frac{A_f}{A_o} \eta_f \right) h_a \tag{20}$$

The continuous fin was divided into rectangular fins due to the symmetry of the temperature field in the continuous fin, fig. 2. The fin efficiency η_f was determined assuming that the air-side heat transfer coefficient h_a is constant. The surface temperature of the fin T_f and the average surface temperature of the $\overline{T}_f$ were calculated by the finite element method using the software ANSYS v.16. The thermal conductivity of the aluminum fin was k_f = 207 W/mK. The calculations were carried out for the air-side heat transfer coefficient h_a varying from 5 W/mK to 300 W/m^{2}K with a 5 W/m^{2}K step. The temperature of the fin base T_b was assumed to be 100 ºC. Temperature distributions on the fin surface for heat transfer coefficients of 10 and 90 W/m^{2}K are depicted in fig. 3. The analysis of the results presented in fig. 3 shows that the temperature of the fin decreases with the increase in the air-side heat transfer coefficient h_a. The fin efficiency η_f calculated for different heat transfer coefficients h_a using the ANSYS v.16 were approximated using the least squares method to obtain:

$$\eta_f = \frac{0.999882 + 0.0003515 h_a}{1 + 0.0021342 h_a}, \quad 0 \le h_a \le 300 \tag{21}$$

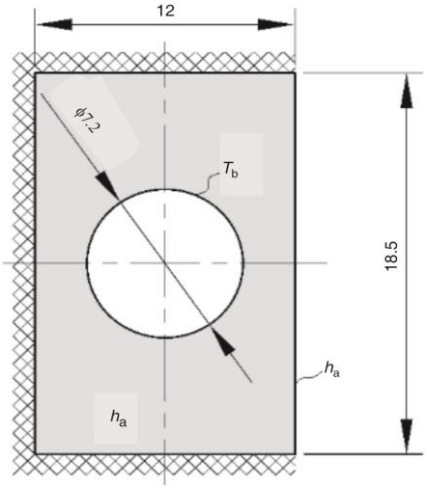

Figure 2. Rectangular fin into which a continuous fin was divided; the lower, upper, and left side surfaces are thermally insulated

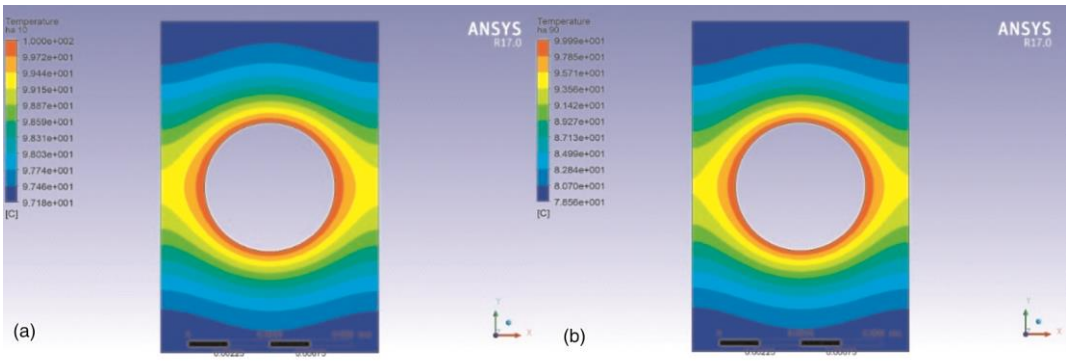

Figure 3. Temperature distributions on the fin surface for various heat transfer coefficients; (a) h_a = 10, (b) h_a = 90

Air-side heat transfer correlation

The Nusselt number on the air side was assumed in the following form:

$$\mathrm{Nu}_a = x_1 \mathrm{Re}_a^{x_2} \mathrm{Pr}_a^{1/3}, \quad 225 \le \mathrm{Re}_a \le 560 \tag{22}$$

The parameters x_1 and x_2 were determined based on the experimental data. The hydraulic diameter on the air side of the investigated heat exchanger was d_a = 1.95 mm. The formula proposed by Kays and London was used [1] to calculate the diameter d_a. The air-side Reynolds number was defined as $\mathrm{Re_a} = w_{\max} d_a / \nu_a$, where $w_{\max}$ is the air velocity in the minimum free flow area. The maximum air velocity $w_{\max}$ occurring within the in-line tube rows is:

$$w_{\max} = \frac{s\, p_1}{\left(s-\delta_{\mathrm{f}}\right)\left(p_1-d_o\right)} \frac{\bar{T}_{am}+273}{T'_{am}+273}\; w_0 \tag{23}$$

where w_0 is the air velocity upstream of the heat exchanger. The tubes in the radiator were arranged inline. Thus, $w_{\max}$ was the air velocity in the narrowest cross-section between two neighboring tubes located in the same row. All physical air properties in eq. (23) were evaluated at the average temperature $\bar{T}_{am} = \left(T'_{am} + T''_{am}\right)/2$.

Liquid-side heat transfer correlation

When operating the heat exchanger in a wide range of loads, the flow regime inside the tubes can be laminar, transitional or turbulent. The heat transfer coefficient for the laminar flow on the waterside depends on the assumed boundary condition on the tube surface. It is possible to set a constant tube wall temperature or a constant heat flux. In the case of tubular cross-flow heat exchangers, better compatibility with experimental results was obtained assuming a constant heat flux at the inner surface of the tubes. Fluid temperature variations in the tubular cross-flow heat exchanger are similar to changes in fluid temperatures that occur in counter-flow heat exchangers. The difference between the temperatures of both fluids is almost constant over the length of the entire heat exchanger. It can, therefore, be assumed that the heat flux at the inner surface of the tubes is constant. First, heat transfer correlations for laminar flow are presented. The average Nusselt number, $\mathrm{Nu}_{m,q}$, for hydraulically and thermally developing laminar fluid-flow in a tube with the uniform wall heat flux was used. The following formula recommended by the VDI Heat Atlas [6] was applied:

$$\mathrm{Nu}_{m,q} = \left[\mathrm{Nu}_{m,q,1}^3 + 0.6^3 + \left(\mathrm{Nu}_{m,q,2} - 0.6\right)^3 + \mathrm{Nu}_{m,q,3}^3\right]^{1/3}, \quad \mathrm{Re_w} \le \mathrm{Re}_{w,trb} \tag{24}$$

The limit value of the Reynolds number, $\mathrm{Re}_{w,trb}$, in which the laminar flow ends, and the transitional starts, is usually taken as 2300 or 2100. The symbol $\mathrm{Nu}_{m,q,1}$ in eq. (24) denotes the mean Nusselt number for hydrodynamically and thermally fully developed flow:

$$\mathrm{Nu}_{m,q,1} = 48/11 = 4.364, \quad \mathrm{Re_w} \le \mathrm{Re}_{w,trb} \tag{25}$$

The Leveque solution [3] $\mathrm{Nu}_{m.q.2}$ denotes the mean Nusselt number for hydrodynamically and thermally fully developed flow over the plate with a linear temperature profile in the fluid and constant heat flux at the wall surface:

$$\mathrm{Nu}_{m,q,2} = 3^{1/3}\Gamma\left(\frac{2}{3}\right)\left[\mathrm{Re_w}\,\mathrm{Pr_w}\left(\frac{d_{\mathrm{in}}}{L}\right)\right]^{1/3} = 1.9530\left[\mathrm{Re_w}\,\mathrm{Pr_w}\left(\frac{d_{\mathrm{in}}}{L}\right)\right]^{1/3}, \quad \mathrm{Re_w} \le \mathrm{Re}_{w,trb} \tag{26}$$

The Nusselt number, $\mathrm{Nu}_{m.q.3}$, appearing in the correlation developed for a tube with a constant wall heat flux is given by:

$$\mathrm{Nu}_{m,q,3} = 0.924\,\mathrm{Pr_w^{1/3}}\left[\mathrm{Re_w}\left(\frac{d_{\mathrm{in}}}{L}\right)\right]^{1/2}, \quad \mathrm{Re_w} \le \mathrm{Re}_{w,trb} \tag{27}$$

The relationship (27) was obtained by an approximation of Nusselt numbers obtained from a numerical solution of the momentum and energy conservation equations assuming a uniform velocity and temperature profiles at the inlet of the tube.

Taler [11] determined the Nusselt number for the turbulent flow in the tube as a function of Prandtl and Reynolds numbers by integrating the energy conservation equation assuming a radial velocity distribution determined experimentally. The relationship proposed by Taler in [11] was generalized to the following form [12]:

$$\mathrm{Nu_w} = \mathrm{Nu}_{m,q}\left(\mathrm{Re}_{\mathrm{w},trb}\right) + \frac{\frac{\xi_\mathrm{w}}{8}\left(\mathrm{Re_w} - \mathrm{Re}_{\mathrm{w},trb}\right)\mathrm{Pr_w^{1.008}}}{1.084 + 12.4\sqrt{\frac{\xi_\mathrm{w}}{8}}\left(\mathrm{Pr_w^{2/3}} - 1\right)}\left[1 + \left(\frac{d_\mathrm{in}}{L}\right)^{2/3}\right], \quad \begin{matrix}\mathrm{Re}_{\mathrm{w},trb} \le \mathrm{Re_w} \le 10^6 \\ 0.1 \le \mathrm{Pr_w} \le 1000,\ \frac{d_\mathrm{in}}{L} \le 1\end{matrix} \tag{28}$$

The water-side Reynolds number $\mathrm{Re_w} = w_w d_\mathrm{in}/\nu_w$ is based on the inner diameter of the circular tube. The physical properties of the water were determined at the mean temperature $\bar{T}_w = \left(T_w' + T_w''\right)/2$.

In the relationship (28) there is a Reynolds number, $\mathrm{Re}_{\mathrm{w},trb}$, at which the transitional flow begins. Usually $\mathrm{Re}_{\mathrm{w},trb} = 2100$ or $\mathrm{Re}_{\mathrm{w},trb} = 2300$ is adopted. In this paper $\mathrm{Re}_{\mathrm{w},trb} = 2100$ was taken. The heat transfer correlation (28) can also be used when the transitional flow regime starts at other values of the Reynolds number [7, 8]. The water-side correlation $\mathrm{Nu_w} = f(\mathrm{Re_w}, \mathrm{Pr_w})$ was assumed for the investigated heat exchanger in the form similar to the correlation (28) valid for flow in straight tubes:

$$\mathrm{Nu_w} = x_3 + \frac{\frac{\xi}{8}\left(\mathrm{Re_w} - \mathrm{Re}_{\mathrm{w},trb}\right)\mathrm{Pr_w^{1.008}}}{1.084 + 12.4\sqrt{\frac{\xi}{8}}\left(\mathrm{Pr_w^{2/3}} - 1\right)}\left[1 + \left(\frac{d_\mathrm{in}}{L}\right)^{2/3}\right] \tag{29}$$

$$2100 \le \mathrm{Re_w} \le 18000, \quad 2.6 \le \mathrm{Pr_w} \le 3.9, \quad \frac{d_\mathrm{in}}{L} = \frac{6.2}{520}$$

The calculations were carried out for $\mathrm{Re}_{\mathrm{w},trb} = 2100$. The unknown parameter x_3 in formula (29) corresponds to the average Nusselt number, $\mathrm{Nu}_{m,q}$, in eq. (28). The parameter x_3 was determined by the least squares method using experimental data.

For $\mathrm{Re}_{\mathrm{w},trb} = 2100$, the friction factor ξ_w in eqs. (28) and (29) is given by a linear function:

$$\xi_\mathrm{w} = 0.030476 + 1.45216 \cdot 10^{-5}\left(\mathrm{Re_w} - 2100\right), \quad 2.1 \cdot 10^3 \le \mathrm{Re_w} \le 3 \cdot 10^3 \tag{30}$$

In the turbulent flow regime, the formula proposed by Taler [9] was used to calculate the friction factor, ξ_w:

$$\xi_\mathrm{w} = \left(1.2776 \log \mathrm{Re_w} - 0.406\right)^{-2.246}, \quad \mathrm{Re}_{\mathrm{w},trb} \le \mathrm{Re_w} \le 10^6 \tag{31}$$

Experimental validation of the mathematical model of the heat exchanger at low loads

Air was forced through the open-loop wind tunnel by a variable speed axial fan [10, 11]. The air-flow passed the whole front cross-section of the heat exchanger. The angular velocity of the fan was changing using a frequency inverter. The hot water was supplied to the radiator from the thermostatically controlled storage tank of 0.8 [$\mathrm{m^3}$] capacities by the centrif-

ugal pump with a frequency inverter. The water-flow rate was measured with a turbine flow meter that was calibrated using a weighing tank. The water volume flow rate was additionally measured using a rotameter. The water temperature at the inlet and exit of the radiator was measured using pre-calibrated *K*-type thermocouples. Air was forced through the open-loop wind tunnel by a variable speed axial fan. The air-flow passed the whole front cross-section of the car radiator. The water volume flow rate was additionally measured using a rotameter. The correlation for the Nusselt number, Nu_a, correlation for the Nusselt number, Nu_w, on the water side, and heat-flow rate, $\dot{Q}_w$, transferred from the hot water to the cold air were determined based on flow and thermal measurements of the car radiator. The following values of parameters were obtained for $\mathrm{Re}_{w,trb} = 2100$ by the least squares method using 70 data points:

$$x_1 = 0.5012,\ x_2 = 0.4137,\quad x_3 = 10.4923 \tag{32}$$

The heat-flow rate $\dot{Q}_{w,calc}$ transferred from the water to air was calculated:

$$\dot{Q}_{w,calc} = \dot{V}_w \rho_w \big|_{T_w'} \bar{c}_w \left(T_w' - T_w''\right) \tag{33}$$

where $\dot{V}_w$ is the volume flow rate measured at the inlet of the heat exchanger, T_w' – the measured temperature at the inlet of the heat exchanger, T_w'' – the calculated temperature at the outlet of the heat exchanger, $\bar{c}_w$ – mean specific heat capacity in the range from T_w'' to T_w'.

The temperature T_w'' was evaluated using the eq. (14). The air-side Nusselt number, Nu_a, was calculated using the correlation (30) with the parameter values x_1 and x_2 given by eq. (32) and the water-side Nusselt number, Nu_w, was obtained from the empirical correlation (29) with x_3 given by eq. (32) or by the semi-empirical formula (32). If the Reynolds number, Re_w, is less than 2100, the water-side heat transfer coefficient was calculated using the relationship (24).

The measured volumetric flow rate, $\dot{V}_w$, at the inlet of the heat exchanger, as well as the measured inlet water temperature, T_w', and the outlet temperature of the water, T_w'', were used for calculating the heat-flow rate:

$$\dot{Q}_{w,\mathrm{exp}} = \dot{V}_w \rho_w \big|_{T_w'} \bar{c}_w \left[T_w' - \left(T_w''\right)^{\mathrm{meas}} \right] \tag{34}$$

The symbol $\bar{c}_w$ in eq. (34) means specific heat of the water between T_w'' and T_w'. The relative difference ε_Q between the calculated heat-flow rate $\dot{Q}_{w,\mathrm{calc}}$ and the heat-flow rate $\dot{Q}_{w,\mathrm{exp}}$ was determined: $\varepsilon_Q = 100(\dot{Q}_{w,\mathrm{calc}} - \dot{Q}_{w,\mathrm{exp}}) / \dot{Q}_{w,\mathrm{calc}}$. The comparison of the calculated and measured heat-flow rate is shown in fig. 4. From the analysis of the results shown in figs. 4(a) and 4(b) it can be seen that the results of the calculations agree very well with the results of the measurements.

Conclusions

A new mathematical model of a car radiator considering laminar, transitional, and turbulent flow regime in tubes was derived and validated experimentally. The semi-empirical and empirical liquid-side correlations ensure the continuity of the Nusselt number at the transition from laminar to transition and from the transition to turbulent flow. The liquid flow regime in tubes can vary from laminar through transitional to turbulent, and *vice versa*. The heat transfer coefficient on the inner surface of the tube is a continuous function of the Reynolds number without sudden variations during the change of the laminar to transition or transition to the turbulent flow regime. The heat-flow rates calculated using the *P*-NTU method agreed very well with the heat-flow rates determined experimentally. Due to the continuity of variations in the water-side heat transfer coefficient, the fluid temperature at the outlet of the

heat exchanger or the heat-flow rate transferred from hot to the cold fluid can be adjusted smoothly by changing the rotational speed of the pump, *i. e*., by changing the volumetric flow rate of the liquid.

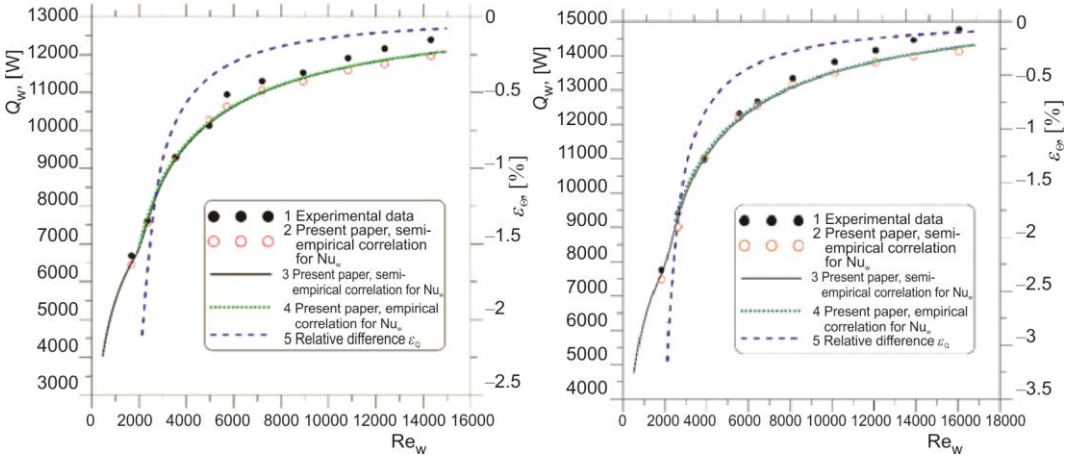

Figure. 4. Heat-flow rate determined experimentally with the heat-flow rate obtained using P-NTU method in the Reynolds number range 500 ≤ $\mathbf{Re_w}$ ≤ 18000; (a) $\bar{w}_0 = 2.27$ **m/s,** $\bar{T}'_{am} = 8.78$ **°C,** $\bar{T}'_w = 61.70$ **°C, (b)** $\bar{w}_0 = 2.27$ **m/s,** $\bar{T}'_{am} = 8.24$ **°C,** $\bar{T}'_w = 70.56$ **°C;** *1 – heat-flow rate* $\dot{Q}_{w,\mathrm{exp}}$ *determined experimentally, 2 – heat-flow rate* $\dot{Q}_{w,\mathrm{calc}}$ *calculated using the P-NTU method with semi-empirical correlation (32) for* Nu_w*, 3 – heat-flow rate* $\dot{Q}_3 = \dot{Q}_{w,\mathrm{calc}}$ *calculated using the P-NTU method and semi-empirical relationship (28) for* Nu_w *using the mean values of measured quantities* $\bar{w}_0$, $\bar{T}'_{am}$, $\bar{T}'_w$, *and* $\mathrm{Nu}_{m,q}\big|_{\mathrm{Re}_{w,trb}=2100} = 9.62$, *4 – heat-flow rate* $\dot{Q}_4 = \dot{Q}_{w,calc}$ *calculated using the P-NTU method and empirical relationship (29 for* Nu_w *with the parameters given by eq. (32) using the mean values of measured quantities* $\bar{w}_0$, $\bar{T}'_{am}$, $\bar{T}'_w$, *and* $x_3 = 10.49$, *5 – relative difference* ε_Q *between* $\dot{Q}_3$ *and* $\dot{Q}_4$ $[\varepsilon_Q = 100(\dot{Q}_3 - \dot{Q}_4)/\dot{Q}_3]$

Nomenclature

A_{bf} – outer surface of the bare tube between fins per one fin pitch, [m^2]
A_f – heat transfer area of the fin, [m^2]
A_in, A_o – inner and outer surface of the bare tube, [m^2]
c_p – specific heat at constant pressure, [Jkg^{-1}K^{-1}]
d_a – hydraulic diameter of air-flow passages, [m]
d_in, d_o – inner and outer diameter of the tube, [m]
h – heat transfer coefficient, [Wm^{-2}K^{-1}]
h_o – effective heat transfer coefficient considering fin efficiency based on the outer surface area of the bare tube, [Wm^{-2}K^{-1}]
H_ch – radiator height, [m]
k – thermal conductivity, [Wm^{-2}K^{-1}] H_ch
L – tube length, [m]
L_ch – width of the radiator, [m]
$\dot{m}_a$ – air mass rate in the automobile radiator, [kgs^{-1}]
$\dot{m}_w$ – water mass rate in the automobile radiator, [kgs^{-1}]
n – total number of tubes in one row of the heat exchanger (= $n_u + n_l$)
n_u, n_l – number of tubes in one tube row in the lower (second) pass and in the upper (first) pass
N_a, N_w – number of transfer units for the air and water side, respectively
$\mathrm{Nu}_{m,q}$ – mean Nusselt number for laminar flow in the tube for constant heat wall flux
$\mathrm{Nu_a}$, $\mathrm{Nu_w}$ – air and water side Nusselt number (= $h_a d_a/k_a$) and (= $h_w d_\mathrm{in}/k_w$)
p_1, p_2 – transversal and longitudinal pitch of tube arrangement, [m]
P_w – water-side effectiveness of the heat exchanger
$\mathrm{Pr_a}$, $\mathrm{Pr_w}$ – air and water side Prandtl number (= $\mu_a c_p/k_a$) and (= $\mu_w c_{p,w}/k_w$)
$\mathrm{Re_a}$, $\mathrm{Re_w}$ – air and water side Reynolds number (= $w_\mathrm{max} d_a/\nu_\mathrm{a}$) and (= $w_\mathrm{w} d_\mathrm{in}/\nu_\mathrm{w}$)

$\mathrm{Re}_{w,trb}$ – the value of the Reynolds number in which the transitional flow begins
s – fin pitch, [m]
T_{cm} – outlet temperature of the water downstream of the first pass, [°C]
T'_{am}, T''_{am} – mean inlet and outlet temperature of the air, [°C]
T'_w, T''_w – water inlet and outlet temperature, respectively, [°C]
U_o – overall heat transfer coefficient referred to the outer surface area of the bare tube, [$\mathrm{Wm^{-2}K^{-1}}$]
$\dot{V}_w$ – water volume flow rate at the inlet of the heat exchanger, [l/h] or [$\mathrm{m^3s^{-1}}$]
w_w – water velocity in the tube, [$\mathrm{ms^{-1}}$]
w_0 – average frontal flow velocity (air velocity before the heat exchanger), [$\mathrm{ms^{-1}}$]
$w_{\max}$ – maximum axial velocity in the minimum free flow area, [$\mathrm{ms^{-1}}$]
W_{ch} – thickness of the radiator, (=$2p_2$), [m]

Greek symbols

Γ – gamma function
δ_f – fin thickness, [m]
δ_t – tube wall thickness, [m]
ε_Q – relative difference between the calculated and experimentally determined heat-flow rate
μ – dynamic viscosity, [Pa·s]
η_f – fin efficiency
ν – kinematic viscosity, [$\mathrm{m^2s^{-1}}$]
ξ – Darcy-Weisbach friction factor
ρ – fluid density, [$\mathrm{kgm^{-3}}$]

Subscripts

a – air
f – fin
in – inner
l – lower (second) pass
p – at constant pressure
t – tube
u – upper (first) pass
w –water

Superscripts

Meas –measured
– – mean,
′ – inlet,
″ – outlet

References

[1] Kays, W. M., London, A. L., *Compact Heat Exchangers*, 3rd ed., Krieger, Malabar, Florida, USA, 1998
[2] Kuppan, T., *Heat Exchanger Design Handbook*, 2nd ed., CRC-Taylor and Francis Group, Boca Raton, Fla., USA, 2013
[3] Taler, D., *Numerical Modeling and Experimental Testing of Heat Exchangers*, Springer International Publishing, Berlin-Heidelberg, 2019
[4] Taler, D., Mathematical Modeling and Control of Plate Fin and Tube Heat Exchangers, *Energy Convers. Manage, 96* (2015), May, pp. 452-462
[5] Taler, D., Simple Power-Type Heat Transfer Correlations for Turbulent Pipe Flow in Tubes, *J. Therm. Sci., 26* (2017), 4, pp. 339-348
[6] Gnielinski, V., Forced Convection in Tubes, in: *VDI Heat Atlas*, Springer-Vieweg, Berlin-Heidelberg, 2013, Chapter G1, pp. 785-792
[7] Ghajar, A. J., Tam, L. M., Heat Transfer Measurements and Correlations in the Transition Region for a Circular Tube with Three Different Inlet Configurations, *Exp. Ther. Fluid Sci., 8* (1994), Jan., pp. 79-90
[8] Everts, M., Meyer, J. P., Heat Transfer of Developing and Fully Developed Flow in Smooth Horizontal Tubes in the Transitional Flow Regime, *Int. J. Heat Mass Transf., 117* (2018), Feb., pp. 1331- 1351
[9] Taler, D., A New Heat Transfer Correlation for Transition and Turbulent Fluid-flow in Tubes, *Int. J. Therm. Sci., 108* (2016), Oct., pp. 108-122
[10] Taler, D., Mathematical Modelling and Experimental Study of Heat Transfer in a Low-Duty Air- Cooled Heat Exchanger, *Energy Convers. Manage., 159* (2018), Mar., pp. 232-243
[11] Taler, D., Taler, J., Prediction of Heat Transfer Correlations in a Low-Loaded Plate-Fin-and-Tube Heat Exchanger Based on Flow-Thermal Tests, *Appl. Therm. Eng., 148* (2019), Feb., pp. 641-649
[12] Taler, D., Experimental Determination of Correlations for Average Heat Transfer Coefficients in Heat Exchangers on Both Fluid Sides, *Heat Mass Transfer, 49* (2013), 8, pp. 1125-1139

Paper submitted: March 12, 2019
Paper revised: April 18, 2019
Paper accepted: May 14, 2019